

Seasonal Variability of Ice Motion for Hubbard and Valerie Glaciers, Alaska

Courtney Bayer,^{1,2} Wesley Van Wychen,¹ Anna Wendleder³ and Brittany Main^{1,4}

(Received 8 March 2024; accepted in revised form 10 September 2024)

ABSTRACT. Hubbard Glacier is a large fast-flowing tidewater-terminating glacier in the St. Elias Mountains and is connected at its terminus to Valerie Glacier. Although Hubbard Glacier has been shown to experience large intra-annual velocity changes and a long-term deceleration, previous seasonality studies have had limited timescale without a dense record of motion. Valerie Glacier's variability has also been understudied, with only one study reporting its seasonal behaviour. The goal of this study was to combine ITS_LIVE, RADARSAT-2, RADARSAT Constellation Mission, and TerraSAR-X/TanDEM-X derived velocity data to create the densest record of motion ever constructed for Hubbard and Valerie glaciers from July 2013-April 2022 in order to explore seasonal velocity variability of both glaciers. Air temperature (NCEP-NCAR Reanalysis) was used to estimate surface melt on the glaciers, which was explored as a potential driver for seasonal velocity changes. Valerie Glacier had a seasonal pattern of fast flow in May, with minimum flow between August-November before accelerating again. Hubbard Glacier displayed a unique seasonal pattern that has not been previously observed on this glacier, with two periods of fast motion: one in May and one in December-February. It is inferred that the spring peaks and late summer/fall minimums on both glaciers are due to meltwater reaching the glacier bed and influencing the subglacial hydrology. The cause of the winter peak and slight velocity drop before the spring peak on Hubbard Glacier has not been determined and should be a topic for future studies, although it is hypothesized to be influenced by its geometry.

Keywords: glaciers; ice dynamics; remote sensing; synthetic aperture radar (SAR); seasonality; climate change; melt; subglacial hydrology

¹ Department of Geography and Environmental Management, University of Waterloo, 200 University Avenue West, Waterloo, Ontario N2L 3D1, Canada; and Meteorological Research Division, Environment and Climate Change Canada, 2121 route Transcanadienne, Dorval, Québec H9P 1J3, Canada

² Corresponding author: courtney.bayer@uwaterloo.ca

³ German Aerospace Centre (DLR), Oberpfaffenhofen, Germany

⁴ Department of Geography, Environment and Geomatics, University of Ottawa

INTRODUCTION AND STUDY SITE

Hubbard Glacier, which originates on Mount Logan's flank at 5959 m (Yukon, Canada) and shares névés and divides with other valley glaciers (such as Kaskawulsh and Logan glaciers), flows >120 km to sea level where it terminates in Disenchantment Bay and Russel Fjord (Yakutat Bay, Alaska) (Fig. 1; Clarke & Holdsworth, 2002; Ritchie et al., 2008; Stearns et al., 2015). It is significant globally as the largest tidewater glacier outside of the poles, with a grounded calving front previously measured to be 11.4 km wide (Meier & Post, 1987; Trabant et al., 2003; Ritchie et al., 2008). Valerie Glacier is a smaller adjacent tributary glacier of Hubbard Glacier, contributing ice into the western edge of Hubbard Glacier's terminus and with a medial moraine between the two glaciers marking their separation (Fig. 1; Mayo, 1988; Ritchie et al., 2008).

Understanding glacier dynamics and how they are evolving for Hubbard and Valerie glaciers is important because it can assist in the improvement of mass balance projections for mountain glaciers, which are limited due to tidewater glacier dynamics not being resolved or understood well (Burgess et al., 2013a). Improving the models can ultimately improve our current understanding of the glaciers' impact on sea level rise. Hubbard Glacier is known for its high velocities and is one out of 12 fast-flowing glacial systems in Alaska identified by Burgess et al. (2013a) with velocities higher than 1 m/d over much of its length due its linkage to high accumulation rates (Burgess et al., 2013a; Waechter et al., 2015; Van Wychen et al., 2018). Although long-term velocity trends on Hubbard Glacier have been difficult to determine because of sparse measurements and large seasonal variation in flow speeds (Stearns et al., 2015), Hubbard Glacier was found to have decelerated from 7.7 m/d in 1978 to 6.0 m/d in 1997 when seasonal variability was removed (Trabant et al., 2003). Broadly, glacier dynamics in Alaska are known to vary interannually, and winter velocities have shown synchronicity throughout the region, which suggests that Alaskan glaciers likely have a common hydrological mechanism driving velocity changes (Burgess et al., 2013b). In support of this idea, Yang et al. (2022) found that different glacier types within the Kenai Peninsula in Alaska showed similar seasonal flow patterns, suggested to be from regional-scale meteorological processes.

In terms of inter-annual velocity changes, Stearns et al. (2015) found that Hubbard Glacier experienced significant variability in flow speeds, ranging from ~4.1 to ~14 m/d, with the faster flow occurring over most regions of Hubbard Glacier's terminus in April/May and the slowest flow in October/November. Similarly, Trabant et al. (2003) determined large seasonal variability in Hubbard Glacier's terminal lobe of up to ~2 m/d, with maximum flow speeds observed in May and June and minimum flow speeds in September and November. These general patterns of variability in ice motion follow the usual seasonality in Alaskan tidewater and land-terminating glaciers (Stearns

et al., 2015; Armstrong et al., 2017). However, despite the work of Stearns et al. (2015) and Trabant et al. (2003), and the known large variability of flow speeds observed on Hubbard Glacier, the characterization of the seasonality of glacier motion for Hubbard glacier remains largely unresolved.

In terms of Valerie Glacier, much of the previous research has been related to pulsing activity (in 1986, August 1993-August 1995, and July 2000-September 2002), where velocities reached higher than ~36 m/d in 1986 (Mayo, 1988; Mayo, 1989; Ritchie et al., 2008). Few studies have investigated the seasonal flow patterns of Valerie Glacier, although Trabant et al. (1991) analyzed Valerie Glacier's velocity from ~1986-1989, which found large seasonal variations (flow speeds near the confluence to Hubbard Glacier in this period ranged from ~2.74 m/d to ~5.48 m/d). Stearns et al. (2015) investigated seasonality at different sections along Hubbard Glacier's terminus and found the region with ice flowing in from Valerie Glacier had a slightly different pattern than other regions of Hubbard Glacier's terminus, with the highest velocities in July/August. A long-term flow pattern of Valerie Glacier was not reported in previous work.

Over the past few decades, remote sensing data has become increasingly available with the launch of new sensors. For example, RADARSAT-2 and TerraSAR-X launched in 2007 (Government of Canada, 2021; Airbus Defence and Space, 2014), TanDEM-X in 2010 (Airbus Defence and Space, 2014), Sentinel-1A in 2014, Sentinel-1B in 2016 (The European Space Agency, 2021), and RADARSAT Constellation mission in 2019 (Government of Canada, 2021). With more remote sensing data available, velocity trends of Hubbard and Valerie glaciers can now be resolved in a higher temporal resolution than has been analyzed in the past. Given this background, the goals of this work are to utilize a large catalogue of remote sensing data in order to:

- build a dense record of ice motion for Hubbard and Valerie glaciers that can be used to resolve the seasonality of both glaciers over the last decade;

- utilize records of climate data to explore the seasonal drivers of ice dynamics at Hubbard and Valerie glaciers.

DATA AND METHODS

Velocity Data

GAMMA Remote Sensing Data: Velocity measurements over Hubbard and Valerie glaciers were generated from intensity offset tracking of Synthetic Aperture RADAR (SAR) data (TerraSAR-X/TanDEM-X (TSX/TDX), RADARSAT-2 (R2), and RADARSAT Constellation Mission datasets (RCM) using the GAMMA RS software. The GAMMA software reads SAR Single Look Complex (SLC) images and utilizes an intensity cross correlation algorithm to determine the

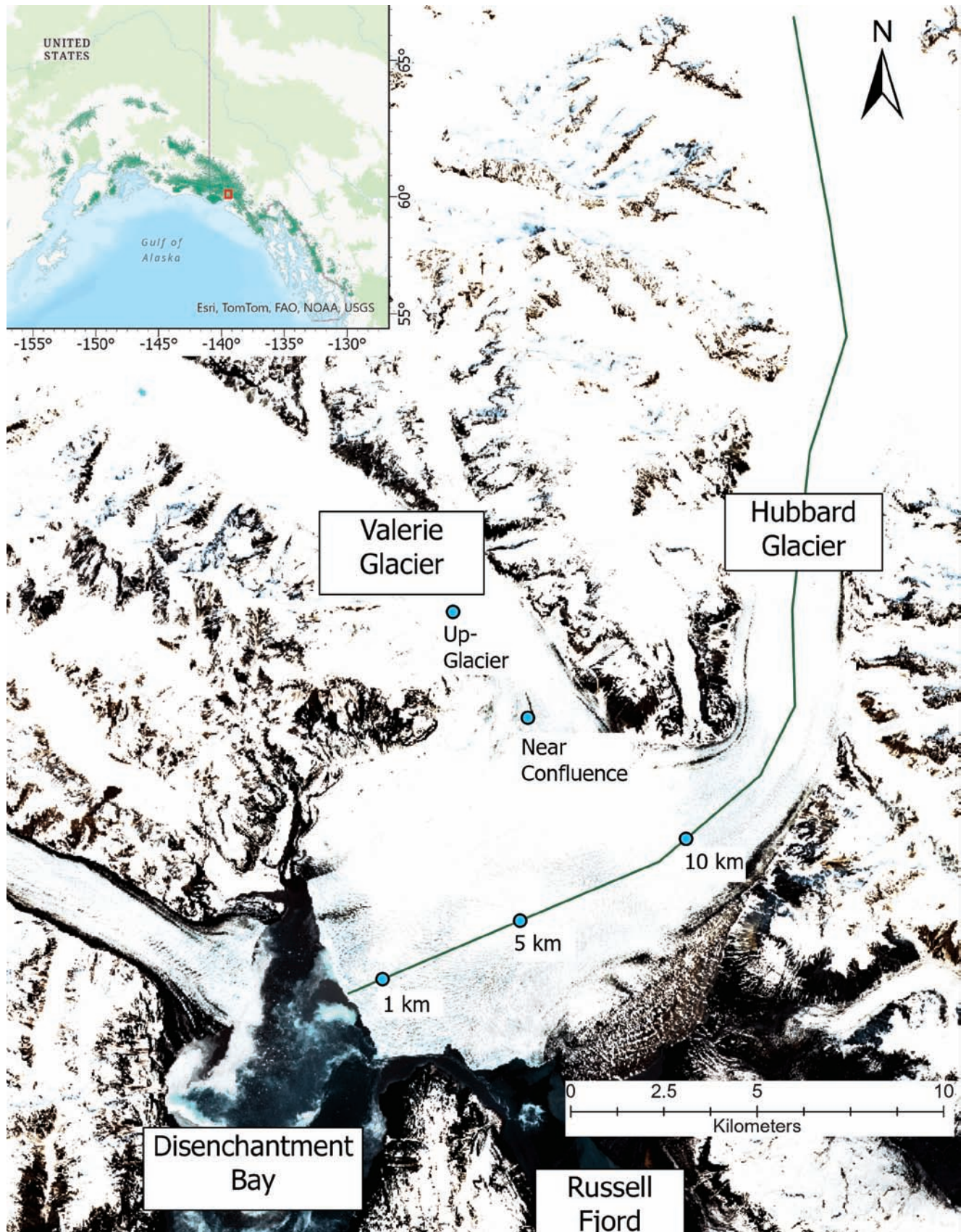


FIG. 1. Hubbard Glacier and Valerie Glacier, with Hubbard Glacier's centerline shown, with locations of data extraction marked at 1 km, 5 km, and 10 km from the terminus (in WGS 1984 UTM Zone 7N). Two points on Valerie Glacier near the confluence of Hubbard Glacier and further up-glacier show the locations of data extraction. Inset: Alaskan glaciated regions (RGI Consortium, 2017) with the red box showing the location of Hubbard Glacier (Esri World Topographic Map, in WGS 1984 Web Mercator). Optical imagery: Sentinel-2 from 11 June 2021.

TABLE 1. Errors of TSX (Samo, 2022), RCM (Van Wychen et al., 2023) and R2 (Van Wychen et al., 2016) used in offset tracking.

| SAR Sensor | Error |
|------------|------------|
| TSX | ~0.016 m/d |
| RCM | ~0.018 m/d |
| R2 | ~0.024 m/d |

displacement between a reference and secondary image (Strozzi et al., 2002). For further details on the creation of velocity products from GAMMA (see the Supplementary Appendix).

Once completed, the GAMMA workflow outputs the calculated displacements in a geocoded GeoTIFF file which are scaled to meters of displacement between the two images that were then transformed to the common unit of m/d.

The uncertainty of glacier velocities from offset tracking is provided in Table 1, with the values of the uncertainty negligible compared to changes to glacier velocity described in the following sections.

ITS_LIVE Data: Pre-derived glacier velocity products for Hubbard and Valerie glaciers were retrieved from NASA MEaSUREs Inter-Mission Time Series of Land Ice Velocity and Elevation (ITS_LIVE) widget (<https://itslive-dashboard.labs.nsidc.org/>; Gardner et al., 2022). This program provides global data on the surface velocity and elevation change of glaciers and ice sheets derived from Sentinel-1, Sentinel-2, and Landsat-7, 8, and 9 image datasets (Gardner et al., 2021). Image-pair velocities of Alaska and Western North America are determined using the autonomous Repeat Image Feature Tracking (auto-RIFT) algorithm between repeated acquisitions, with Sentinel-2 and Landsat satellite imagery used if cloud cover was $\leq 60\%$ (Gardner et al., 2021). Gardner et al. (2018) provides full documentation on the methods used for this dataset and provide an uncertainty estimate of $\sim 0.055\text{--}0.082$ m/d. These products have a pixel resolution of 120 m and were constrained to a time separation between images of 7-30 days, which allowed for a sub-monthly temporal resolution of the dynamics of both Hubbard and Valerie glaciers to be obtained between July 2013 and April 2022. Data is more scarce towards the beginning of the ITS_LIVE record, with the density of velocity products in the dataset increasing at the end of 2016, as a result of the launch of additional sensors (European Space Agency, 2020; European Space Agency, 2021; Gardner et al., 2021; U.S. Geological Survey, 2022).

Hubbard Glacier data was downloaded at three points corresponding to 1 km (60.0137, -139.5069), 5 km (60.027, -139.4402), and 10 km (60.0458, -139.3594) from its terminus along its centerline (determined from manual selection while using optical imagery as a reference) to show how its velocity behaviour changed when moving up-glacier, away from the terminus. Valerie Glacier data was downloaded at two locations, the ‘near confluence’ point (60.0758, -139.4337) and the ‘up-glacier’ point

(60.1018, longitude -139.4687) to evaluate the velocity fluctuations near the confluence of Valerie Glacier and Hubbard Glacier and at a location further removed from the influence of Hubbard Glacier (points shown in Fig. 1).

Glacier Velocity Extraction for Hubbard and Valerie Glaciers: To provide a detailed determination of the seasonal variability of both Hubbard and Valerie glaciers, the velocity data from all sources (ITS_LIVE data and GAMMA RS data) were analyzed at five locations - three locations on Hubbard Glacier and two locations on Valerie Glacier (as described for the ITS_LIVE data) - from July 2013-April 2022. The combined velocity dataset resulted in 1296 velocity samples at Hubbard Glacier’s 1 km location, 1407 velocity samples at Hubbard Glacier’s 5 km location and 923 velocity samples at Hubbard Glacier’s 10 km location. For Valerie Glacier, 1273 velocity samples were obtained confluence location and 994 velocity samples at the up-glacier point.

Melt Analysis

Climate was analyzed using reanalysis data from NCEP-NCAR reanalysis 1 (Kalnay et al., 1996) provided by NOAA PSL, Boulder, Colorado, USA (from <https://psl.noaa.gov/data/gridded/data.ncep.reanalysis.html>). Mean daily surface air temperatures (sigma level 995) were downloaded for 2013-2022, and were used to calculate the number of Positive Degree Day (PDD) sums for each month. The reanalysis surface air temperature products are provided on a $2.5^\circ \times 2.5^\circ$ grid, and the grid cell located at 60, -140 was chosen to capture the climate at Hubbard Glacier (60.045, -139.39). To calculate monthly PDD sums, if the mean surface air temperature of individual days within the month was above 0°C , those values were cumulatively summed.

RESULTS

Spatial Velocity Structure of Hubbard and Valerie Glaciers

Figure 2 provides the general velocity structure of Hubbard and Valerie glaciers. With respect to Hubbard Glacier, higher velocities are found close to its terminus where the glacier front meets the ocean. Moving up-glacier from the terminus, glacier velocities decrease to reach a minimum ~ 5.6 km from the terminus. After this point, velocities increase again and reach a maximum ~ 11.4 km from the terminus, where the glacier is constricted between valley walls and has a relatively steep slope. Although this spatial pattern of ice motion is observed at all times, there is a large amount of temporal variability in glacier motion. Valerie Glacier experiences faster velocities up-glacier, away from its terminus, although large seasonal variations in its velocity are also observed. A further description of the seasonality of both glaciers is provided in the following sections.

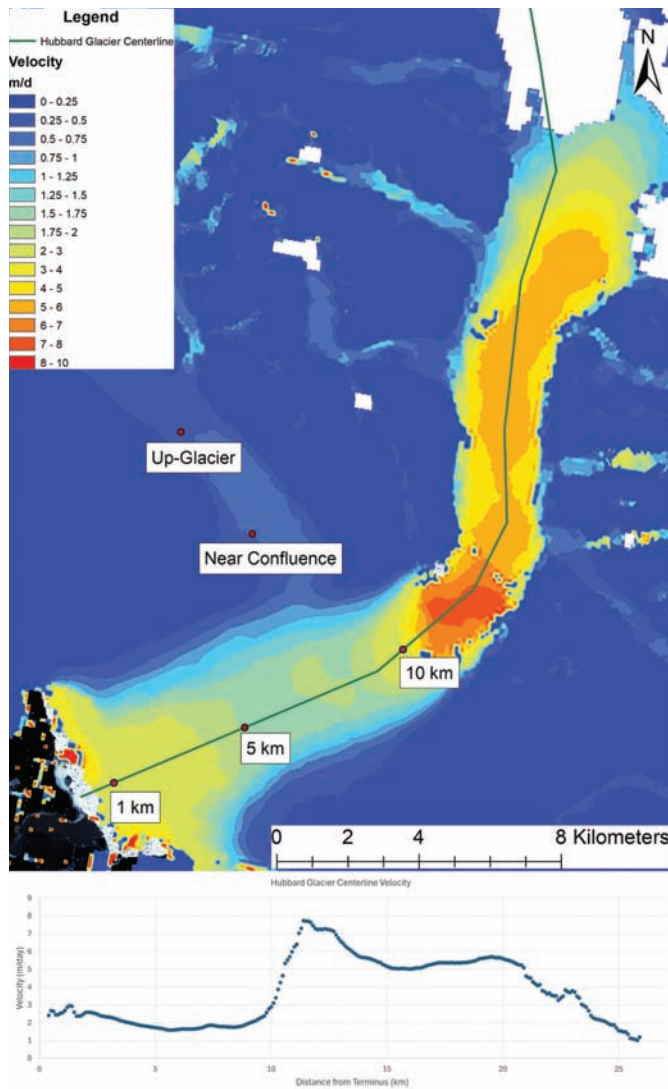


FIG. 2. Glacier velocities of Hubbard and Valerie glaciers from TSX data on 21 August 2015 to 01 September 2015 (optical imagery: Sentinel-2 imagery from 11 June 2021, in WGS 1984 UTM Zone 7N).

Seasonality of Hubbard and Valerie Glaciers

Figure 3a-e presents the velocity structure of Hubbard and Valerie glaciers from July 2013 to May 2022 from the extracted remote sensing derived displacement maps at five distinct locations (identified with teal dots on Fig. 1). Seasonality of glacier motion is much more detailed after 2016 due to the wider availability of glacier velocity maps after this time, and 2022 data does not cover the full year. As such, the description and quantification of glacier motion that follows focuses on the time period of January 2017 to January 2022.

Seasonally, two velocity peaks and two velocity drops were observed each year at all three locations on Hubbard Glacier (Fig. 3a-c). This velocity pattern was most evident at the location 1 km from the terminus, with the same pattern, albeit with a much smaller amplitude, also observed at the 5 km and 10 km points. Therefore, this discussion is focused on the 1 km point. At this location, one velocity peak

occurred in the winter months (varying between December and February in different years) before velocities dropped slightly and reached a minimum between the end of January-April (again, varying between years). At 1 km from the terminus, maximum velocities during this winter peak occurred in January 2020, when Hubbard Glacier's velocity exceeded ~ 13 m/d. In this study period, the minimum values in the drop after this peak reached lower than ~ 5.0 m/d (as seen in March 2021). The relative decrease between this winter peak and following minimum was generally less than ~ 5.2 m/d, although velocities decreased as much as ~ 7.9 m/d from January-April 2020. Velocities increased after this minimum to a second velocity peak that occurred in the spring (fastest velocities in May), where velocities at 1 km from the terminus reached higher than ~ 9.6 m/d at its maximum (May 2019). After this spring peak, velocities dramatically decreased, with this drop often larger than what occurred after the winter velocity peak, to reach minimum velocities in the late summer/fall (between August-October). These were the slowest velocities of the year, reaching as low as 0.77 m/d at 1 km from the terminus (September 2018). This relative decrease in velocity was always larger than ~ 5.5 m/d and decreased more than ~ 8.2 m/d in 2018. It was variable if the winter peak was higher than the following spring peak each year.

Unlike Hubbard Glacier, Valerie Glacier (Fig. 3d,e) only experienced one seasonal velocity peak and velocity decrease each year. The velocity peak occurred in spring (generally in May) after a gradual acceleration from the winter until this peak. Velocities were observed to reach higher than ~ 4.4 m/d at the near confluence point and ~ 4.8 m/d at the up-glacier point. Following this peak, velocities decrease rapidly until dropping to its minimum velocities, then plateauing at this low flow speed in late the fall, with velocities as low as ~ 0.055 m/d at the near confluence point (September-November) and ~ 0.22 m/d at the up-glacier point (August/September). After the minimum velocities, flow speeds gradually increase until the spring peak was reached again. This pattern was consistent in all years analyzed.

Positive Degree Days and Climate Analysis

Figure 3f shows the PDD sums from 2013-2022, with this analysis also focusing on January 2017-December 2021 to allow for a direct comparison to seasonal velocity trends. The general PDD sum seasonal cycle is described here, although some years may have differences in the timing of increases and decreases of values. Generally, January-March had minimal PDD sums ($<10^{\circ}\text{C}$), with March/April PDD sums increasing but still small ($<25^{\circ}\text{C}$). The increasing PDDs coincides with increasing velocities on Valerie Glacier until its peak velocities around May. Similarly, Hubbard Glacier's velocities began to increase around April until the peak in May. After April, PDD sums continued to increase until the maximum was reached in July/August (maximum values in July 2019 reaching $\sim 370^{\circ}\text{C}$), with minimum velocities following close after

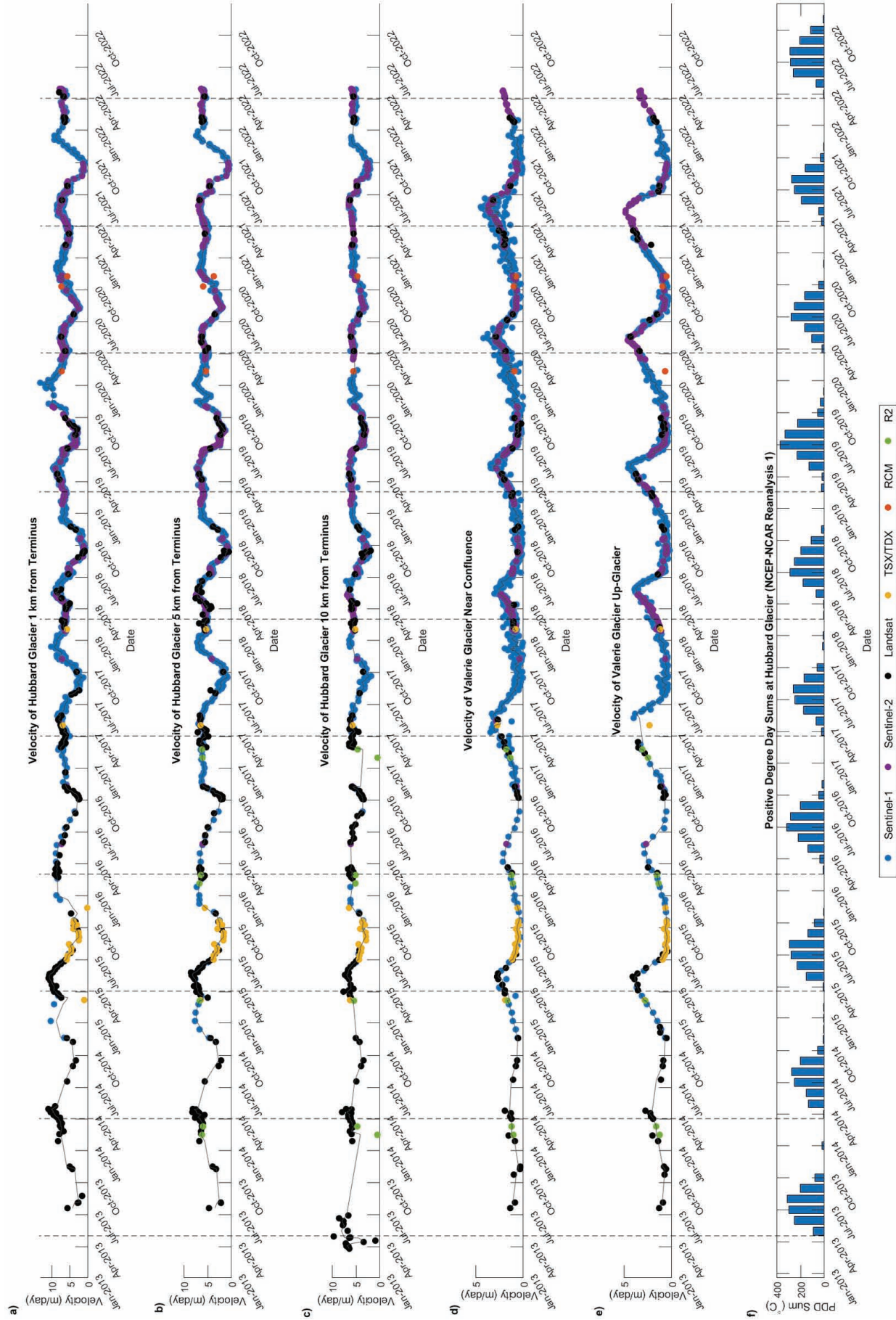


FIG. 3. Velocity of Hubbard Glacier at 1 km (a), 5 km (b) and 10 km (c) from its terminus. The velocity of Valerie Glacier is shown near the confluence point with Hubbard Glacier (d) and further up-glacier (e). To graph the velocity data as a timeseries, a running mean line using $k = 3$ was used. The PDD sums (f) are shown. Point locations are found in Figure 1. TSX/TDX is TerraSAR-X/TanDEM-X, RCM is RADARSAT Constellation Mission, and R2 is RADARSAT-2. The grey dashed lines represent the first spring month with $>5^{\circ}\text{C}$ PDD sum following the minimum winter/spring PDD sum value. RADARSAT Constellation Mission Imagery © Government of Canada (2020), RADARSAT is an official mark of the Canadian Space Agency.

these maximum PDD sum values are reached (August-October for Hubbard Glacier, August-November for Valerie Glacier). After the maximum PDD sums are reached, values begin to decrease but are still relatively high until September/October ($>100^{\circ}\text{C}$). Following this until the end of the year, values keep decreasing and become minimal again around November/December ($<6^{\circ}\text{C}$, although maximum December PDD sum of $\sim 17^{\circ}\text{C}$ occurred in 2017).

DISCUSSION

Seasonality of Hubbard Glacier

Figure 4 displays a general conceptual presentation of the seasonal patterns Hubbard Glacier experienced, including its inferred subglacial hydrology, ice motion, and melt, which are described throughout the following section.

The late-spring/early-summer velocity speedup on Hubbard Glacier follows the expected velocity response of a glacier to inputs of melt water into an inefficient subglacial drainage network (Willis, 1995; Nienow et al., 1998). For example, each year Hubbard Glacier’s velocities increased until a velocity peak was observed in May (Figs. 3a-c, 4) which coincides with the increasing monthly PDD sums throughout the spring/summer (Fig. 3f). The velocity peak coinciding with melt suggests that early in the melt season (April–May each year; Fig. 3f), when PDD sums were increasing from month-to-month, the generated melt was drained to the glacier bed and into an inefficient sub-glacial drainage network. Input of melt to the bed led to increased glacier velocities (Figs. 3a-c, 4) as the glacier can slide more easily over a well lubricated bed (hard-bedded) or have more bed deformation (soft-bedded) (Willis, 1995).

The velocities of Hubbard Glacier decelerate each year after the May peak and reached the lowest velocities of the year in late summer/fall (Fig. 3a-c) over a period of time when monthly PDD sums were diminishing from their July/August peak until December (Fig. 3f). This evolution in dynamic response to air temperatures and, by proxy surface melt, is likely explained by a switch to an efficient subglacial drainage system that is able to quickly transport surface meltwater through the englacial and subglacial drainage networks (Fig. 4). The efficient subglacial drainage system leads to less lubrication between the glacier and its bed, thereby increasing friction or decreasing till deformation, and causing flow speeds to decrease (Willis, 1995). This hypothesis is supported by the findings of Ritchie et al. (2008) who examined imagery and found that 50% of summers had embayments located on the terminus at Disenchantment Bay. These were likely caused by increased calving at the terminus front as a result of increased subglacial drainage, where from the summer to the fall the openings were visible, but were closed during the winter (Ritchie et al., 2008).

Each year, the flow speeds of Hubbard Glacier rebounded relatively quickly towards the winter peak after the annual

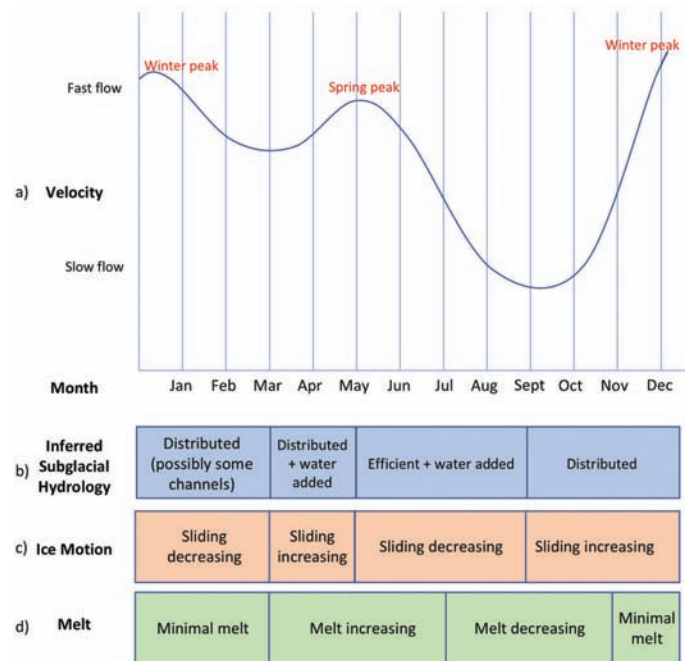


FIG. 4. Hubbard Glacier’s hypothesized seasonal patterns. The velocity plot shows the fast winter and spring peaks, and the minimums after each peak (a). The subglacial hydrology is described as distributed or efficient (b), ice motion describes if sliding of the glacier on its bed is increasing or decreasing (c), and melt describes how much melt was observed from the PDD sums (d).

velocity minimum was observed in late summer/fall (Fig. 3a-c). To account for this behaviour, it is argued that the overall fast movement of Hubbard Glacier may quickly cause ice deformation and destruction of the efficient subglacial channels that were developed during the summer, causing the distributed sub-glacial system to rapidly reform again (Nienow et al., 1998). The only way for efficient channels to enlarge or be maintained is if the amount of surface meltwater reaches the bed in appreciable quantities (Willis, 1995). Although PDD sums were greater than zero over this period, albeit diminishing from month to month after July/August each year (Fig. 3f), it is unlikely the amount of melt that was generated was sufficient to maintain this efficient subglacial drainage network.

An interesting aspect of Hubbard Glacier is the relatively high flow speeds that were reached during the winter season (between December-February annually; Figs. 3a-c, 4). From a purely remote sensing-based approach, it is difficult to determine the exact cause of the high winter velocities, but a few theories are presented here. The cause of the winter speedup may be due to trapped water existing at high pressures in the subglacial channels, which can decrease friction at the bed (hard-bed) or facilitate bed deformation (soft-bed) and allow sliding to occur throughout the winter (Willis, 1995). It is also possible that increasing glacier thickness due to snow accumulation can increase deformation and/or basal motion, as was observed on Hintereisferner in Austria, which had slower summer velocities than annual speeds, even with little to no meltwater reaching the bed (Blümcke & Finsterwalder, 1905; Willis, 1995). Another possibility is that liquid precipitation in the fall is

reaching the bed of the glacier and increasing winter flow speeds (Yang et al., 2022). However, there are other possible mechanisms that can cause velocity changes (for example, ocean-ice interaction at the calving front, draining of supraglacial lakes, etc.) that cannot be dismissed until further exploration of Hubbard Glacier's velocity pattern allows the cause to be determined.

The high winter velocities of Hubbard Glacier were consistent in all years in this study, but this pattern was not found on Valerie Glacier (Fig. 3d-e), meaning that the process that was causing high flow rates for Hubbard Glacier at this time is likely influenced by the geometry of Hubbard Glacier. If the process was being driven solely by climate conditions, a similar winter velocity peak for Valerie Glacier would also be expected. The geometry of Hubbard and Valerie glaciers causing differences in seasonal flow speeds is supported by the hypothesis of Enderlin et al. (2018) stating that seasonal variations in flow speeds and basal drag are controlled through a glacier's geometry, which has a connection to its subglacial hydrology. Although the study by Enderlin et al. (2018) was focusing on the geometry of retreating tidewater glaciers, it is possible this also applies to advancing tidewater glaciers due to the evidence shown in this study.

After the velocity peak between December-February on Hubbard Glacier, the velocities dropped slightly to reach a low point between February and April. Similar to the winter velocity peak, the cause of the velocity decrease was not possible to determine using remote sensing. However, it is possible that the subglacial hydrologic network may have experienced a minor re-organization where water found preferential paths to create some channels, which lead to the drop in velocity. Alternatively, if precipitation events were the cause of the winter velocity increase (as put forth by Yang et al. (2022)), then this decrease in flow occurs because in the late winter/early spring water from rainfall no longer reaches the bed.

It is important to note that the seasonal variations on Hubbard Glacier are most pronounced 1 km from the terminus, meaning this process may be linked to ocean processes at the calving front. It is also possible that the increased velocity variability further down-glacier may be caused by pressure variations from variations in surface water input (Willis, 1995). These pressure variations can be the result of higher melt rates in the lower ablation area, having thinner snowpacks further down-glacier (this decreases the attenuating influence), and an increased chance of the creation of an efficient englacial hydrologic system down-glacier (Willis, 1995). However, this efficient system was stated to be from lower ice-deformation rates in the down-glacier region, which was not observed on Hubbard Glacier (Willis, 1995). The water pressure down-glacier is more probable to be a higher percentage of the ice overburden pressure compared to regions further up-glacier (Willis, 1995).

Comparison of Hubbard Glacier's Seasonal Flow with Previous Studies

The large amount of velocity data provided in this study has provided a significant improvement on the understanding of the seasonality of flow of Hubbard Glacier compared to previous studies. Previous studies by Stearns et al. (2015) and Trabant et al. (2003) both found highest flows in spring, and slowest flows in fall, however, neither of those works described the fast overall motion during the winter months that is reported here. The differences in the seasonal pattern may arise from our study using data with a higher temporal resolution, as the velocity data used in Stearns et al. (2015) may be averaging out the winter velocity peak due to their winter velocities being determined through averaging fall to spring data. As well, Trabant et al. (2003) analyzed two different velocity datasets, one of a fixed location consisting of 22 image pairs, and one set on a moving location with 11 velocity measurements. Through the limited amount of speed measurements, this pattern may not have been captured in the Trabant et al. (2003) study. The amount of data used in this study was not available until SAR become popular and an increased number of sensors were launched, allowing this study to characterize seasonality on Hubbard and Valerie glaciers in a way that was not possible in the past.

Moon et al. (2014) provided one of the largest characterizations of seasonal patterns of ice motion using records of tidewater glacier motion albeit from Greenland, with the characterizations further supported by Solgaard et al. (2022). Hubbard Glacier's seasonal flow (Fig. 4) does not fit exactly into any of the categories identified by Moon et al. (2014), which further demonstrates the uniqueness of this behaviour. This difference might arise from the number of observations used, where the glaciers studied by Moon et al. (2014) only had 3-6 measurements annually from 2009-2013, although a few glaciers had more frequent measurements. Kehrl et al. (2017) found that Kangerlussuaq Glacier in Greenland behaved similarly to what is presented here for Hubbard Glacier, with a velocity peak in the summer due to temperatures increasing meltwater that reaching the bed, and a velocity peak in the winter due to retreat of the iceshelf.

Columbia and Post glaciers are tidewater glaciers located in Alaska that also experience interannual velocity changes in a similar way to Hubbard Glacier, with seasonal velocity patterns assumed to be caused by changes to the subglacial hydrological network, and both glaciers had larger variations in flow speeds closer their termini than further up-glacier (Enderlin et al., 2018). Enderlin et al. (2018) used 89 velocity fields from 2012-2016, and despite the similarities of Columbia Glacier and Hubbard Glacier, the first half of their study period showed Columbia and Post glaciers generally having maximum velocities in May/June, then a rapid drop in velocities to reach minimum velocities in October/November (Enderlin et al., 2018). However, in 2014, Post Glacier showed unusual flow behaviour with

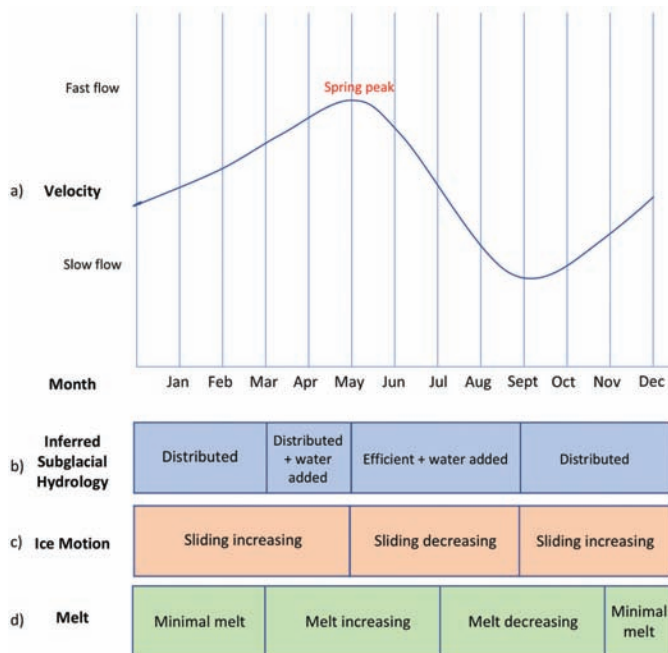


FIG. 5. Valerie Glacier's hypothesized seasonal patterns. The velocity plot shows the maximum velocity in the spring, followed by minimum velocities in the fall (a). The inferred subglacial hydrology describes if the system is distributed or efficient (b), ice motion describes if the glacier is increasing or decreasing sliding on its bed (c), and melt describes how much melt was observed from the PDD sums (d).

increased flow speeds and two velocity peaks, which is similar to the pattern we observed on Hubbard Glacier (Enderlin et al., 2018). The behaviour of Post Glacier differed from Hubbard Glacier as that anomalous year also had much higher flow speeds than average before dropping to much lower flow speeds than average for the 2015 minimum, which is not observed on Hubbard Glacier as the pattern of two velocity peaks occurred in all years analyzed from January 2017 to January 2022 (Enderlin et al., 2018). Although there are differences between the results of Enderlin et al. (2018) and what is reported here, it would be interesting for future work to study Columbia and Post glaciers in the same resolution of Hubbard and Valerie glaciers to determine if Hubbard Glacier's unique seasonal pattern is also observed on similar glaciers (i.e. large size, tidewater) when the density of data allows the observation. The seasonal behaviour of Hubbard Glacier would have previously been considered unusual for Alaska, although it is likely that previous studies never observed this seasonal pattern due to their data density being much sparser compared to what is presented here.

Yang et al. (2022) found that within the Kenai Peninsula in Alaska, the glaciers flowed in a similar way to that observed by Hubbard Glacier, with a velocity peak in May, decreasing velocities until a September/October minimum, and increasing velocities until a secondary peak in November. This velocity pattern was observed across many glaciers and different glacier types (land-terminating, tidewater-terminating, lake-terminating), although with varying amplitudes (Yang et al., 2022).

Similar to what is presented here, Yang et al. (2022) suggest changing subglacial drainage systems from meltwater to be the cause of the spring speedup and following slowdown. However, Yang et al. (2022) attribute regional-scale high precipitation rates that occur in the fall as the cause of increased glacier motion in the early winter across the entire peninsula. Precipitation was not analyzed for Hubbard and Valerie glaciers, although, it is possible that regional-scale precipitation is the cause of the winter speedup on Hubbard Glacier. However, analyzing the effect of precipitation on these glaciers should be the focus of future work, as neighbouring and connected Valerie Glacier does not show the same pattern of winter ice motion as Hubbard Glacier (possibly due to differences in glacier geometry, as discussed in the previous section), contrasts with the synchronous short-term speed patterns of glaciers across the Kenai Peninsula (Yang et al., 2022). However, this pattern of seasonal glacier behaviour may be more common in Alaska than previous studies have shown, as a temporally dense velocity dataset throughout the entire year was needed to display this on Hubbard Glacier, and with similar findings now shown on Post Glacier (Enderlin et al., 2018) and in the Kenai Peninsula (Yang et al., 2022).

Seasonality of Valerie Glacier

Valerie Glacier's seasonal behaviour is summarized in Figure 5, showing the seasonal changes to its velocity, inferred subglacial hydrology, ice motion, and melt. Valerie Glacier showed a very traditional melt-induced flow variability signal and can be explained in the same way as the spring peak on Hubbard Glacier; through changes to subglacial hydrology (Willis, 1995). The velocities of Valerie Glacier increased until the spring peak was reached, coincident with warming temperatures that increased melt that is inferred to be delivered to the glacier bed and increased basal water pressure. During this time, the discharge of water out from beneath the glacier is likely low to moderate, leading to the lubrication of the bed of the glacier and a short-term increase in flow speeds (Willis, 1995). As the melt season progresses, the distributed network that leads to the spring velocity peak evolved into a channelized/efficient system by the end of the melt season, leading to the termination of fast spring velocities, and was followed by intermediate summer velocities and minimum velocities in later summer/fall (Nienow et al., 1998; Armstrong et al., 2017). The melt driving velocity change is supported by the distribution of PDD sums (Fig. 3f), with peak melt conditions occurring with velocity minimums. Valerie Glacier experienced Gradually increasing velocities following the minimum fall velocities, suggesting the efficient channels evolved back to a distributed system because of ice deformation (Nienow et al., 1998).

This behaviour differed from Hubbard Glacier as Valerie Glacier only experienced one velocity peak and one velocity drop each year, unlike Hubbard Glacier that had two velocity peaks and drops. The winter velocity

peak observed on Hubbard Glacier did not exist on Valerie Glacier, although they both had a spring peak around the same time each year, and late summer/fall minimums. Valerie Glacier's fastest velocities were in the spring, as opposed to Hubbard Glacier's fastest velocities commonly observed in the winter. Also, Valerie Glacier did not rebound to faster velocities after its minimum velocities were reached as quickly as Hubbard Glacier did, and in comparison, it had a more gradual speedup until its spring peak was reached again. The slower acceleration of Valerie Glacier may have been caused by its slower velocities than Hubbard Glacier, which would have taken longer to destroy the efficient drainage network.

CONCLUSIONS

This study examined the seasonality of Hubbard and Valerie glaciers at a higher temporal resolution than previously possible and provided the densest velocity record of Hubbard and Valerie glaciers ever created. This record reveals that the seasonal variability of ice flow on Hubbard Glacier increases when moving towards its calving front, and it experiences two velocity peaks and drops throughout the year, one peak in the spring (May) before dropping to minimum velocities in late summer/fall (August-October), peaking again in the winter (December-February), before dropping slightly between February-April. Hubbard Glacier's behaviour is different from that of Valerie Glacier, which experiences one velocity peak in the spring (May) before dropping to minimum flow speeds between August-November. The summertime velocity peak of both glaciers was argued to be caused by rising air temperatures increasing meltwater and raising water pressure at the bed, which allows enhanced basal sliding (Willis, 1995). Once seasonal melt increases enough, efficient channels form, leading to minimum velocities in late summer/fall, generally around when PDD values are decreasing, but still high (Nienow et al., 1998; Armstrong et al., 2017). On both glaciers, it is argued that the efficient drainage channels shift back to a distributed system due to ice deformation, leading to both glaciers speeding up, although Hubbard Glacier at a faster rate than Valerie Glacier, likely due to its faster velocities (Nienow et al., 1998). Although there are similarities between Hubbard and Valerie glaciers and Columbia and Post glaciers, there are differences between their seasonality, whereas similar velocity patterns have been observed in the Kenai Peninsula (Enderlin et al., 2018; Yang et al., 2022). The work by Enderlin et al. (2018), Yang et al. (2022), and this study show that this "double peak" velocity pattern may be more common in Alaska than previously thought.

The cause of this wintertime velocity peak observed on Hubbard Glacier was not determined, but a few methods for fast velocities were hypothesized. First, this may be due to water trapped beneath the glacier, although the method of increased velocities differs depending on if Hubbard Glacier has a hard or soft bed (Willis, 1995). If a hard bed exists, fast winter velocities may result from water increasing lubrication beneath the bed, while if it has a soft bed, it might have fast winter velocities from water causing bed deformation or till failure (Willis, 1995). Second, fast winter velocities may be caused by increased ice deformation and/or basal motion by increased basal deformation and regelation due increasing thickness from snow accumulation (Blümcke & Finsterwalder, 1905; Willis, 1995). Lastly, it is possible that rainwater in the fall increased winter flow speeds (Yang et al., 2022). Due to fast winter velocities not found on neighbouring Valerie Glacier, it is likely the driver of the winter velocity peak is affected by the geometry of Hubbard Glacier. This study can not draw any firm conclusions to the cause of the velocity drop after the winter velocity peak, although it is hypothesized that water may be finding preferential paths and increasing the efficiency of the subglacial drainage before being destroyed by the fast velocities and becoming fully distributed again to reach the spring peak, or due to decreased rainwater input reaching the bed. Future work could focus on the causes of the winter velocity peak and the subsequent velocity drop, as no firm conclusions can currently be made and it is possible that other causes besides the hydrologic network are influencing Hubbard Glacier's seasonal velocity trend (for example, ocean-ice interaction at the calving front or supraglacial lake drainage). It is possible that other glaciers are behaving in a similar way, although their velocity data was not temporally dense enough to see this pattern.

ACKNOWLEDGEMENTS

We acknowledge the support of the Natural Sciences and Engineering Research Council of Canada, [CGS-M to CB and Discovery Grant (RGPIN-02443-2021) to WvW]. Cette recherche a été financée par le Conseil de recherches en sciences naturelles et en génie du Canada (CRSNG), [CGS-M à CB et de subventions à la découverte (RGPIN-02443-2021) à WvW].

We also acknowledge the support of Canada Foundation for Innovation (John Evan's Leadership Fund), the Ontario Research Fund, Environment and Climate Change Canada – Climate Research Division, the University of Waterloo, ArcticNet Network of Centres of Excellence Canada. The TerraSAR-X data are available through the DLR (©DLR 2023).

REFERENCES

- Airbus Defence and Space 2014. TerraSAR-X Image Product Guide.
https://www.engesat.com.br/wp-content/uploads/r459_9_201408_tsxx-itd-ma-0009_tsx-productguide_i2.00.pdf
- Armstrong, W.H., Anderson, R.S., and Fahnestock, M.A. 2017. Spatial patterns of summer speedup on South Central Alaska glaciers. *Geophysical Research Letters* 44(18):9379–9388.
<https://doi.org/10.1002/2017GL074370>
- Blümcke, A. and Finsterwalder, S. 1905. Zeitliche Änderungen in der Geschwindigkeit der Gletscherbewegung. *Sitzungsberichte der mathematisch-physikalischen Klasse der Kgl. Bayerischen Akademie der Wissenschaften zu München* 35(1):109–13131.
- Burgess, E., Forster, R., and Larsen, C. 2013a. Flow velocities of Alaskan glaciers. *Nature Communications* 4(2146).
<https://doi.org/10.1038/ncomms3146>
- Burgess, E.W., Larsen, C.F., and Forster, R.R. 2013b. Summer melt regulates winter glacier flow speeds throughout Alaska. *Geophysical Research Letters* 40(23):6160–6164.
<https://doi.org/10.1002/2013GL058228>
- Clarke, G.K.C., and Holdworth, G. 2002. Glaciers of the St. Elias Mountains. In *Satellite image atlas of glaciers of the world: glaciers of North America-glaciers of Canada*. (U.S. Geological Survey Professional Paper, 1386-J-1). [Williams, R.S. Jr & Ferrigno, J.G. (eds.)] U.S. Geological Survey, Reston, VA: J301-J328. The European Space Agency 2021. About Copernicus Sentinel-1... [infographic].
<https://sentinels.copernicus.eu/documents/247904/4603794/Sentinel-1-infographic.pdf>
- Enderlin, E.M., O'Neel, S., Bartholomaeus, T.C., and Joughin, I. 2018. Evolving environmental and geometric controls on Columbia Glacier's continued retreat. *Journal of Geophysical Research: Earth Surface* 123(7):1528–1545.
<https://doi.org/10.1029/2017JF004541>
- Gardner, A.S., Fahnestock, M.A., and Scambos, T.A. 2022. MEaSURES ITS_LIVE Landsat Image-Pair Glacier and Ice Sheet Surface Velocities. (NSIDC-0775, Version 1) [Data Set]. Boulder, Colorado USA. NASA National Snow and Ice Data Center Distributed Active Archive Center. Date accessed 30-11-2022 and 14-12-2023.
<https://doi.org/10.5067/IMR9D3PEI28U>
- Gardner, A.S., Fahnestock, M.A., and Scambos, T.A. 2021. MEaSURES ITS_LIVE Landsat image pair glacier and ice sheet surface velocities: Version 1 (Beta).
http://its-live-data.jpl.nasa.gov/s3.amazonaws.com/documentation/ITS_LIVE-Landsat-Scene-Pair-Velocities-v01.pdf
- Gardner, A.S., Moholdt, G., Scambos, T., Fahnestock, M., Ligtenberg, S., van den Broeke, M., and Nilsson, J. 2018. Increased West Antarctic and unchanged East Antarctic ice discharge over the last 7 years. *The Cryosphere* 12:521–547.
<https://doi.org/10.5194/tc-12-521-2018>
- Government of Canada 2021, January 12. RADARSAT satellites: Technical comparison.
<https://www.asc-csa.gc.ca/eng/satellites/radarsat/technical-features/radarsat-comparison.asp>
- Kehrl, L.M., Joughin, I., Shean, D.E., Floricioiu, D., and Krieger, L. 2017. Seasonal and interannual variabilities in terminus position, glacier velocity, and surface elevation at Helheim and Kangerlussuaq Glaciers from 2009 to 2016. *Journal of Geophysical Research: Earth Surface* 122(9):1635–1652.
<https://doi.org/10.1002/2016JF004133>
- Main, B., Copland, L., Smeda, B., Kochtitzky, W., Samsonov, S., Dudley, J., Skidmore, M., Dow, C., Van Wychen, W. Medrzycka, D., Higgs, E., and Mingo, L. 2022. Terminus changes of Kaskawulsh Glacier, Yukon, under a warming climate: Retreat, thinning, slowdown and modified proglacial lake geometry. *Journal of Glaciology* 69(276):936–952.
<https://doi.org/10.1017/jog.2022.114>
- Mayo, L.R. 1988. Advance of Hubbard Glacier and closure of Russell Fiord, Alaska—environmental effects and hazards in the Yakutat area. In *Geologic studies in Alaska (U.S. Geological Survey during 1987)*. [Galloway, J.P., and Hamilton, T.D. (eds.)] U.S. Geological Survey Circular 1016:4–16
- Mayo, L. 1989. Advance of Hubbard Glacier and 1986 Outburst of Russell Fiord, Alaska. USA. *Annals of Glaciology* 13:189–194.
<https://doi.org/10.3189/S0260305500007874>
- Meier, M.F. and Post, A. 1987. Fast tidewater glaciers. *Journal of Geophysical Research* 92(B9):9051–9058.
<https://doi.org/10.1029/JB092iB09p09051>
- Moon, T., Joughin, I., Smith, B., van den Broeke, M.R., van der Berg, W.J., Noël, B., and Usher, M. 2014. Distinct patterns of seasonal Greenland glacier velocity. *Geophysical Research Letters* 41(20):7209–7216.
<https://doi.org/10.1002/2014GL061836>
- Nienow, P., Sharp, M., and Willis, I. 1998. Seasonal changes in the morphology of the subglacial drainage system, Haut Glacier D'Arolla, Switzerland. *Earth Surface Processes and Landforms* 23(9):825–843.
[https://doi.org/10.1002/\(SICI\)1096-9837\(199809\)23:9<825::AID-ESP893>3.0.CO;2-2](https://doi.org/10.1002/(SICI)1096-9837(199809)23:9<825::AID-ESP893>3.0.CO;2-2)
- RGI Consortium 2017. Randolph Glacier Inventory—A Dataset of Global Glacier Outlines. (NSIDC-0770, Version 6). [Data Set]. Boulder, Colorado USA. National Snow and Ice Data Center. [Alaska]. Date accessed 15-07-2022.
<https://doi.org/10.7265/4m1f-gd79>

- Ritchie, J., Lingle, C., Motyka, R., and Truffer, M. 2008. Seasonal fluctuations in the advance of a tidewater glacier and potential causes: Hubbard Glacier, Alaska, USA. *Journal of Glaciology* 54(186):401–411.
<https://doi.org/10.3189/002214308785836977>
- Samo, L. 2022. Investigation of intra-annual velocity and seasonality of White and Thompson Glaciers, Axel Heiberg Island, Nunavut. [Master's Thesis, University of Waterloo].
<https://dspacemainprd01.lib.uwaterloo.ca/server/api/core/bitstreams/662a40c5-4528-4a1e-aedb-2ec4108825cd/content>
- Solgaard, A.M., Rapp, D., Noël, B.P.Y., and Hvidberg, C.S. 2022. Seasonal patterns of Greenland ice velocity from Sentinel-1 SAR data linked to runoff. *Geophysical Research Letters* 49(24): e2022GL100343.
<https://doi.org/10.1029/2022GL100343>
- Stearns, L.A., Hamilton, G.S., van der Veen, C.J., Finnegan, D.C., O'Neel, S., Scheick, J.B. and Lawson, D.E. 2015. Glaciological and marine controls on terminus dynamics of Hubbard Glacier, southeast Alaska. *Journal of Geophysical Research: Earth Surface* 120(6):1065–1081.
<https://doi.org/10.1002/2014JF003341>
- Strozzi, T., Luckman, A., Murray, T., Wegmuller, U., and Werner, C. L. 2002. Glacier motion estimation using SAR offset-tracking procedures. *IEEE Transactions on Geoscience and Remote Sensing* 40(11):2384–2391.
<https://doi.org/10.1109/TGRS.2002.805079>
- Trabant, D.C., Krimmel, R.M., and Post, A. 1991. A preliminary forecast of the advance of Hubbard Glacier and its influence on Russell Fjord, Alaska. In *Water-Resources Investigations Report 90-4172*. U.S. Geological Survey.
<https://doi.org/10.3133/wri904172>
- Trabant, D., Krimmel, R., Echelmeyer, K., Zirnheld, S., and Elsberg, D. 2003. The slow advance of a calving glacier: Hubbard Glacier, Alaska, U.S.A. *Annals of Glaciology* 36:45–50.
<https://doi.org/10.3189/172756403781816400>
- U.S. Geological Survey 2022. Landsat 9 Data Users Handbook Version 1.0.
https://d9-wret.s3.us-west-2.amazonaws.com/assets/palladium/production/s3fs-public/media/files/LSDS-2082_L9-Data-Users-Handbook_v1.pdf
- Van Wychen, W., Copland, L., Jiskoot, H., Gray, L., Sharp, M., and Burgess, D. 2018. Surface Velocities of Glaciers in Western Canada from Speckle-Tracking of ALOS PALSAR and RADARSAT-2 data. *Canadian Journal of Remote Sensing* 44(1):57–66.
<https://doi.org/10.1080/07038992.2018.1433529>
- Van Wychen, W., Bayer, C., Copland, L., Brummell, E., and Dow, C. 2023. Radarsat Constellation Mission Derived Winter Glacier Velocities for the St. Elias Icefield, Yukon/Alaska: 2022 and 2023. *Canadian Journal of Remote Sensing* 49(1).
<https://doi.org/10.1080/07038992.2023.2264395>
- Van Wychen, W., Davis, J., Burgess, D.O., Copland, L., Gray, L., Sharp, M., and Mortimer, C. 2016. Characterizing interannual variability of glacier dynamics and dynamic discharge (1999–2015) for the ice masses of Ellesmere and Axel Heiberg Islands, Nunavut, Canada. *Journal of Geophysical Research Earth Surface* 121(1):39–63.
<https://doi.org/10.1002/2015JF003708>
- Van Wychen, W., Copland, L., Gray, L., Burgess, D., Danielson, B., and Sharp, M. 2012. Spatial and temporal variation of ice motion and ice flux from Devon Ice Cap, Nunavut, Canada. *Journal of Glaciology* 58(210):657–664.
<https://doi.org/10.3189/2012JoG11J164>
- Willis, I.C. 1995. Intra-annual variations in glacier motion: a review. *Progress in Physical Geography: Earth and Environment* 19(1):61–106.
<https://doi.org/10.1177/030913339501900104>
- Yang, R., Hock, R., Kang, S., Guo, W., Shangguan, D., Jiang, X., and Zhang, Q. 2022. Glacier surface speed variations on the Kenai Peninsula, Alaska, 2014-2019. *JGR Earth Surface* 127(3): e2022JF006599.
<https://doi.org/10.1029/2022JF006599>